

## Nonlinear response studies and corrections for a liquid crystal spatial light modulator

RAVINDER KUMAR BANYAL\* and B RAGHAVENDRA PRASAD

Indian Institute of Astrophysics, Bangalore 560 034, India

\*Corresponding author. E-mail: banyal@iiap.res.in

MS received 20 May 2009; revised 4 February 2010; accepted 24 February 2010

**Abstract.** The nonlinear response of light transmission characteristics of a liquid crystal (LC) spatial light modulator (SLM) is studied. The results show that the device exhibits a wide range of variations with different control parameters and input settings. Experiments were performed to obtain intensity modulation that is best described by either power-law or sigmoidal functions. Based on the inverse transformation, an appropriate pre-processing scheme for electrically addressed input gray-scale images, particularly important in several optical processing and imaging applications, is suggested. Further, the necessity to compensate the SLM image nonlinearities in a volume holographic data storage and retrieval system is demonstrated.

**Keywords.** Liquid crystal spatial light modulator; holographic data storage; optical image processing.

**PACS Nos** 42.70.Df; 42.30.-d; 42.70.Ln; 42.40.Pa; 42.40.Ht; 42.25.Bs; 42.79.-e

### 1. Introduction

Liquid crystal (LC) based spatial light modulators (SLM) are electro-optic devices that are capable of modulating the phase, polarization or intensity of light according to a desired spatial and temporal pattern. The initial research in LC technology was driven by the electronic consumer industry aiming to develop various projection displays, computer screens, liquid crystal television [1–5] etc. However, the increasing versatility, advancement in fabrication technology and low cost of LC spatial light modulators (LC-SLM) have led to its use in diverse areas of scientific research ranging from optical correlation, beam steering, matched filtering, polarization control to optical data processing, tweezers, laser projection, dynamic holography, wave-front sensing and correction in adaptive optics system [6–20].

SLM is one of the most important system components in holographic data storage system (HDSS) used for composing an optical data page prior to the storage [21]. While LC-SLM presents a straightforward and practical solution for spatial modulation (amplitude or phase) of light for HDSS system, these are limited both in

terms of spatial resolution and also bit depth that determine the available gray-scale range [22].

The intensity transmitted by the LC cell is influenced by several factors. These include the effect of signal conditioning by the graphics board, the brightness and contrast control settings of the projector and the relative orientation of the polarizer and the analyzer. Therefore, it is imperative to quantify some of these properties in order to optimize the storage performance. Most often there is no *a priori* information about the dependence of intensity and phase modulations on various parameters like brightness and contrast control, threshold voltage, polarization orientation of incident light etc. In this paper, the modulation properties of a commercially available LC-SLM are presented. The SLM response, at various input parameters, would help us to determine an optimum range of operation that is required to suit its usage in HDSS. Therefore, if the SLM is 'biased' to an optimum operating point (governed by relative orientation of the polarizer and the analyzer and appropriate brightness and contrast settings) that lies within the maximum linearity of the response curve, then over a certain gray-level range the SLM will provide a square law mapping of incremental change in incident light amplitude into incremental change of amplitude transmittance.

In this paper, a detailed study of the light transmission characteristics of a commercially available SLM is presented. The experimental results indicate a highly nonlinear (input/output) response of the device. Measured intensity modulation curves are best described by either power-law or sigmoidal functions. Based on the power-law transformation, an appropriate pre-processing of input gray-scale images for page-oriented holographic data storage applications is suggested. Finally, the proof of the concept to improve the SLM image quality is demonstrated in a high fidelity volume holographic data storage and retrieval system implemented in the lab.

## **2. Nonlinearities and corrections**

The nonlinear response of a variety of devices used in display applications can severely degrade the image quality. In order to quantify and correct the device response, the relationship between the input signal and the output signal of the device must be accurately established. Subsequently, this relationship is used to re-map the input signal values to produce a desired output response of the device. The SLM usually consists of densely packed liquid crystal cells arranged in two-dimensional pixel arrays. A coating of transparent electrode allows voltage to be applied across any individual pixel. The nematic LC material that fills the gap between two parallel glass plates has layers of elongated molecules. These molecules show orientational order within the cell having anisotropic optical properties similar to the uniaxial crystals [23]. The light transmission properties of each cell can be controlled using externally applied voltage signal. For all practical purposes, the Jones matrix analysis is suffice to predict the intensity and the phase modulation characteristics of the twisted LC cell [24,25].

Spatial light modulators used in various optical information processing and projection applications also exhibit a certain degree of nonlinearity. Usually the voltage

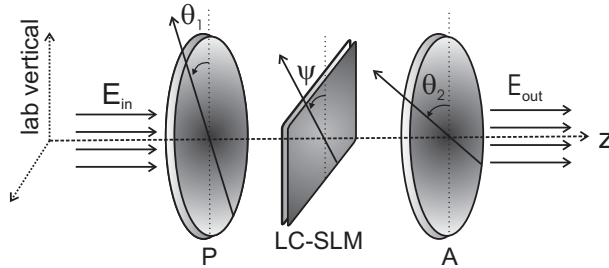


**Figure 1.** Experimental lay-out of the twisted nematic LC-SLM in common projection and display applications.

$V$  applied across a given LC pixel is proportional to the brightness of the image pixel at that location. However, in normal systems, a nonlinearity between applied voltage and the pixel transmittance is always introduced because of the graphics board and the projector electronics. Typically, a digital image with certain gray-level distribution is addressed electrically onto the SLM. The replica of the image is transferred to a plane parallel to the optical beam that is either reflected or transmitted through the LC-SLM panel. Because of SLM nonlinearities, the gray-level replication from the input image to the optical image is never perfect. Various software and/or hardware-based techniques can be used to compensate these nonlinearities. Usually, a look-up table is generated to re-map the gray-level values appropriately. In this paper, the discussion is confined only to software pre-processing of the gray-scale images that is necessary to compensate the SLM nonlinearities.

Mathematically, the spatial domain transformation for an input image and output image can be written as

$$s = \mathcal{T}(r), \quad (1)$$

where  $\mathcal{T}$  is a gray-level transformation which maps the pixel value  $r$  at input image  $X(i, j)$  onto the pixel value  $s$  at output image  $Y(i, j)$ .

In general, any imaging device can be modelled based on its input/output mapping response curves. The SLM response characteristics that we determined experimentally are also in good agreement with the theoretical curves obtained from the model proposed by Lu and Saleh [25].

### 3. Experimental results and discussion

The SLM in our lab is an electrically addressed LC2002 model from HoloEye Photonics. The device consists of a twisted nematic LC panel (Sony LCX016AL-6; active area:  $26.6 \times 20.0 \text{ mm}^2$ ; number of pixels:  $832 \times 624$ ; pixel pitch:  $32 \mu\text{m}$ , type: transmissive,  $\Psi = 45^\circ$ ) and driver electronics that can be plugged directly to the output of the video graphics card of a computer. The user, therefore, does not have direct access to control the input signal and the bias voltage applied to the individual cells of the LC panel. These parameters are controlled indirectly

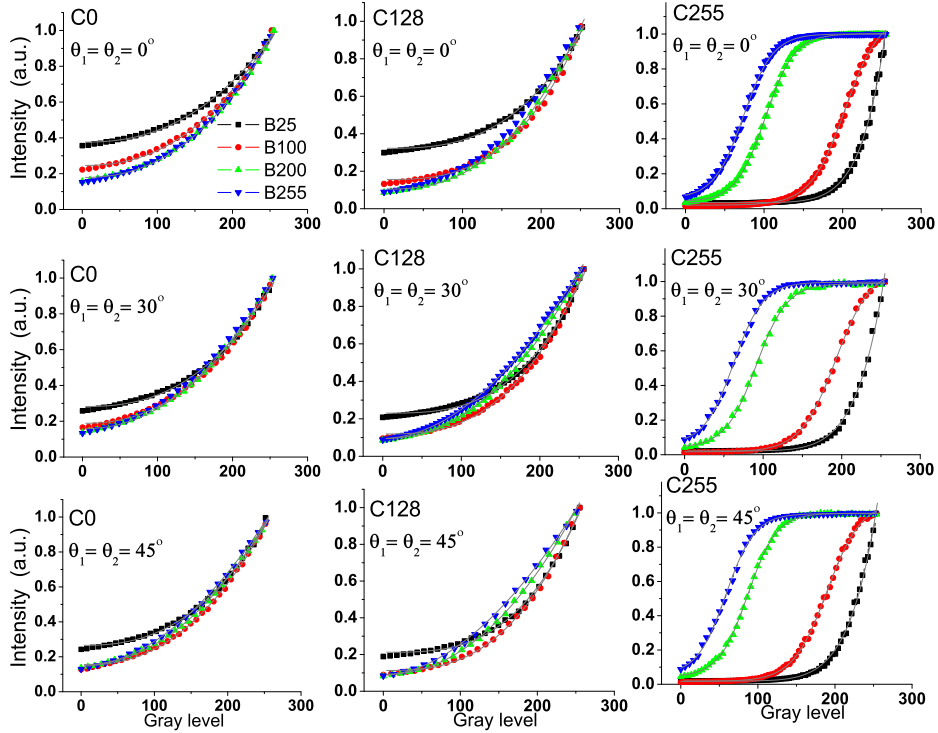


**Figure 2.** Intensity modulation curves in parallel configuration of the polarizer and the analyzer at contrast settings 0, 128 and 255, are designated respectively by C0, C128 and C255. Curves identified with different symbols correspond to brightness settings of 25, 100, 200 and 255, and are designated respectively by B25, B100, B200, B255.

by varying the brightness and contrast settings through the driver software over a range from 0 to 255. However, there is no *a priori* information as to how the brightness and the contrast control settings affect the transmittance properties on the SLM. A common scheme used for studying the modulation properties of the LC-SLM sandwiched between a polarizer (P) and an analyzer (A) is shown in figure 1. Here,  $\theta_1, \theta_2$  and  $\Psi = 45^\circ$  are angles that the axis of polarizer, analyzer and molecular director of the LC cell make with the lab vertical.

### 3.1 Measurement of intensity modulation curves

In this section, the optical transmission properties of LC-SLM studied in the power-on state are described. The light transmittance was studied by electronically addressing the SLM with several homogeneous images. Here, a homogeneous image means the image with one shade, i.e. all the pixels have the same gray-level values.

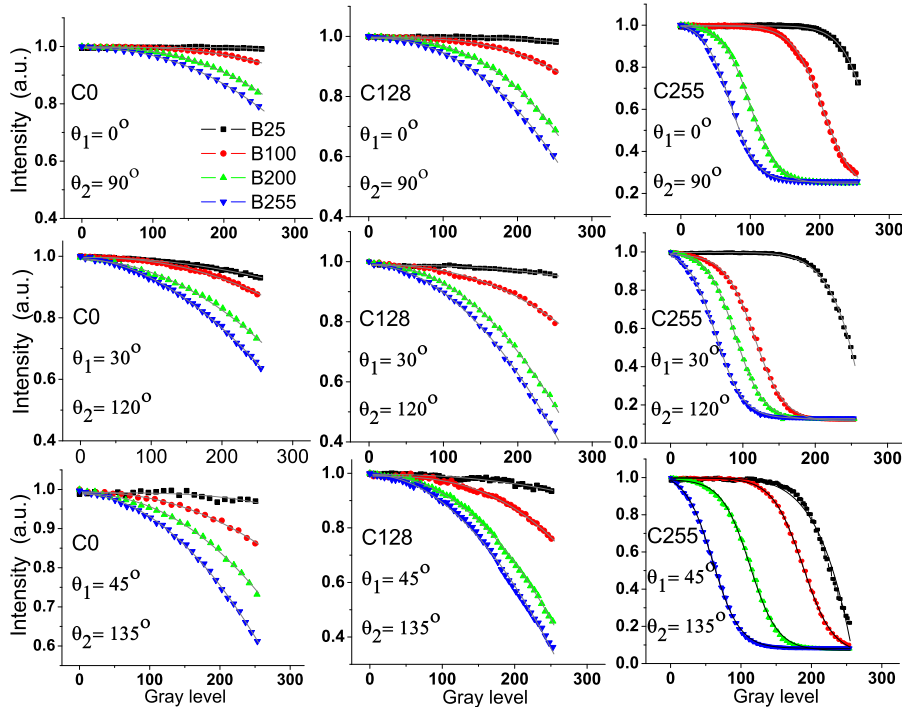


**Figure 3.** Intensity modulation curves in crossed configuration of the polarizer and the analyzer at contrast settings 0, 128 and 255, are designated respectively by C0, C128 and C255. Curves identified with different symbols correspond to different brightness settings B25, B100, B200 and B255.

A computer programme was written to sequentially address a set of 51 homogeneous images with gray level progressively varying from 0 to 255 in steps of 5. An expanded and well-collimated He-Ne laser beam at 632.8 nm illuminated the central portion ( $500 \times 500$  pixels) of LC panel and the variations in transmitted intensity were recorded simultaneously using computer-controlled large area photodetector (Model: 4832-C Multichannel Optical Power Meter; Newport). Experimental measurements were made at several brightness and contrast settings.

Some typical representative intensity modulation curves for the crossed and parallel configurations of the polarizer and analyzer oriented at different angles with respect to lab vertical are shown in figures 2 and 3, respectively. The measured data are represented by different symbols, whereas the thin lines are the nonlinear curve fittings using power-law (eq. (3)) or sigmoidal function (eq. (4)). The nonlinear nature of the transmitted intensity is clearly evident from figures 2 and 3. These figures also indicate how the gray levels in the input image map to gray levels in SLM projected image. To this end, it is instructive to define a parameter of interest, called, intensity modulation depth (IMD) as the difference in the transmitted intensity at the maximum (255) and minimum (0) input gray level, i.e.,

$$\text{IMD} = |T(\text{GL} = 255) - T(\text{GL} = 0)| \times 100\%. \quad (2)$$

Given an input image, the above equation reflects the degree of contrast that can be rendered to SLM output image at different control settings. From practical point of view the configuration that gives an IMD of 100% is most desirable. A brief comparison between figures 2 and 3 shows that the maximum IMD in cross orientation of the polarizer and the analyzer is only about 85%, whereas it is possible to achieve 100% IMD in the parallel configuration. At low brightness and contrast settings ( $<50$ ), the IMD is too poor to render any meaningful contrast to the SLM images. Likewise, the usable gray-scale range at high brightness and contrast setting (e.g. B255 and C255) is relatively small.

For certain range of brightness and contrast settings (e.g. the first two columns in figures 2 and 3), the functional form of transmitted intensity of the SLM is well approximated by the power-law response. On the other hand, the SLM response for brightness  $B > 50$  and contrast = 255 (curves in the 3rd column of each figure) is more appropriately described by the sigmoidal function. In terms of gray-level transformation, the power-law response of the SLM can be expressed as

$$s = a + br^\gamma, \quad (3)$$

where  $a$ ,  $\gamma$  are real positive constants and  $b > 0$  ( $b < 0$ ) for parallel (cross) configuration.

For all cases, it turned out that  $\gamma > 1$ , which implies that the response of LC-SLM is such that it maps a wider range of low input gray levels into a narrow range of output values, and the opposite being true for higher input gray levels. This essentially amounts to decrease in overall brightness and increase in contrast in the bright areas at the expense of the contrast in dark area. The  $\gamma$  values calculated by experimental data fitting using eq. (3) are shown in figures 4a and 4b.

This nonlinear response, characterized by the exponent  $\gamma$  at different brightness and control settings of the SLM, can be corrected by appropriate pre-processing of the input images. The inverse transformation would require that low gray-level ranges is stretched and the higher-level range is compressed. To this end, let the response of SLM for a given configuration be characterized by some  $\gamma$ . Using eq. (3), the inverse power-law transformation can be chosen such that  $s' = r^{1/\gamma}$ .

To demonstrate the effect of nonlinearities, several 8-bit gray-scale images were addressed onto the SLM placed between a crossed polarizer and analyzer. The transmitted images were captured by the CCD camera placed behind the SLM. As shown before, the SLM pixels have a sublinear transmission response at low input gray-level values. The SLM-transmitted images, therefore, appear more darker than the original. For example, figure 5a shows the original ( $128 \times 128$  pixels) image of *Lena* that was addressed onto the SLM without any pre-processing. The darkening effect due to nonlinearities is clearly seen in the SLM transmitted image 5c. Here, the brightness and contrast setting of the SLM was set at 128. This corresponds to  $\gamma \approx 2.5$ . Using the inverse power-law transformation, figure 5a was digitally transformed into figure 5b by up-scaling the region of darker shades in the image. The expected improvement in SLM's response is clearly visible in figure 5d. A small loss in visual image quality in both cases was due to the low quality of polaroid sheets. The CCD images are also somewhat enlarged due to the slight magnification ( $m > 1$ ) of imaging optics.

Nonlinear response studies and corrections

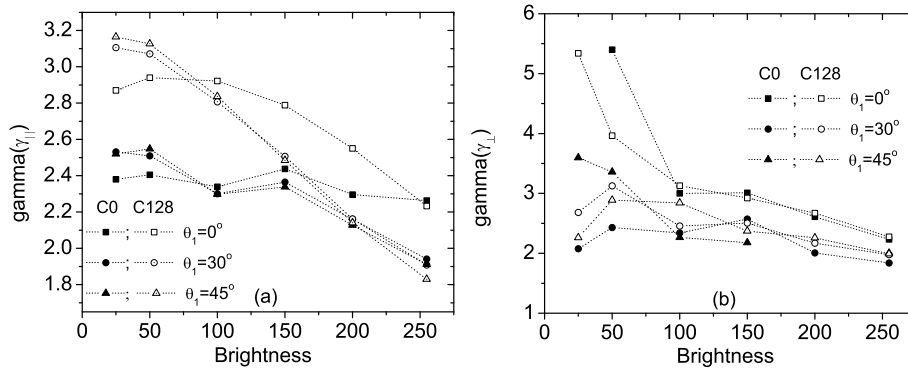


**Figure 4.** Plot of power-law exponent  $\gamma$  vs. brightness control as a function of orientation and contrast settings for (a) the parallel and (b) the crossed configurations. Filled and open symbols corresponding to contrast settings of 0 and 128 are denoted respectively by C0 and C128.



**Figure 5.** (a) Original *Lena* image, (b) transformed image, (c) SLM output for the original image and (d) SLM output for the transformed image captured on CCD.

It is to be noted from figures 3 and 4 that the intensity modulation curves for contrast setting 255 and brightness  $B > 50$  do not follow power-law behaviour. The SLM response in this regime is somewhat similar to  $H$  and  $D$  curves for photographic emulsion that can be described by a sigmoidal function of the form:

$$s = s_b + \frac{s_t - s_b}{1 + \exp[-(r - r_o)/w]}, \quad (4)$$

where  $s_b$  and  $s_t$  are two asymptotic values at small and large  $r$ . The curve crosses over between two asymptotic values in a region of  $r$  whose approximate width is  $w$

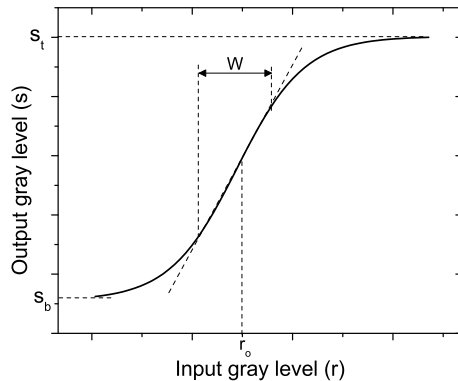


**Figure 6.** Sigmoidal function response of the LC-SLM when contrast  $C = 255$  and brightness  $B > 50$ .

and which is centred around  $r_0$ . Visual representation of these parameters is shown in figure 6.

The best parameter fits of sigmoidal function for the data in figures 2 and 3 are recorded in table 1. The response of LC2002 around  $r_0$  is almost linear, however, the width  $w$  is rather small. Therefore, the usage of SLM in this regime is rather limited, and generally avoided in all applications of practical interest.

### 3.2 High fidelity volume holographic data storage and retrieval

In a volume holographic data storage system, an image carrying coherent laser beam spatially patterned by LC-SLM, optically interferes with another identical plane parallel reference beam. A photorefractive crystal placed in the region of interference, stores the image in the form of refractive index grating. The original image page can be read at later time by illuminating the storage medium with the same reference beam that was used to record it. The diffracted beam which is a replica of the original image data can be captured by a CCD camera or by a photographic film. In light of the work described so far, we have further used the LC-SLM to demonstrate the storage and retrieval of high fidelity holographic image storage. Based on the preceding discussions on intensity modulations, we chose the following settings for the optimum range of the control parameter in our holographic data storage experiment.

- The best operating configuration of SLM that gives reasonably good IMD and sufficiently wider gray-scale range may be expected to occur in the intermediate range (i.e. around B128 and C128) of brightness and contrast settings. Therefore, both the contrast and the brightness settings were fixed at 128. For these settings, the transmission characteristics of the SLM exhibit power-law form. The required pre-processing (the inverse transformation) of the input images is, therefore, relatively easier to accomplish than the high contrast region ( $C = 255$ ) dominated by sigmoidal response.

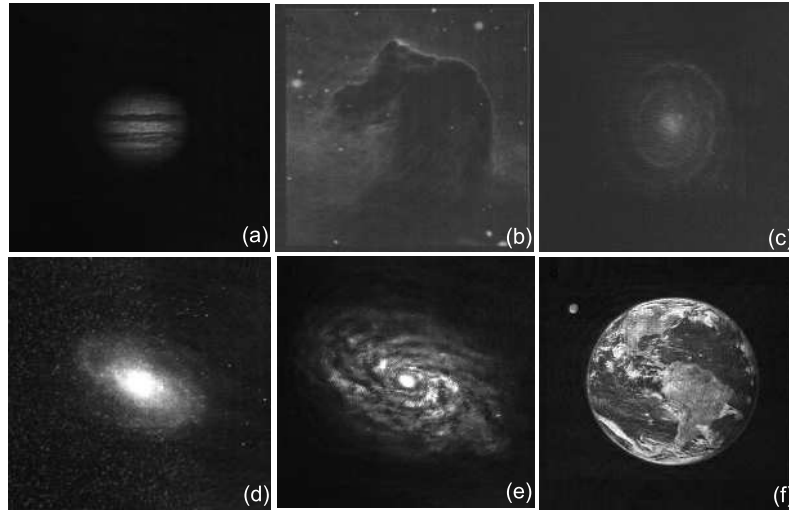


**Figure 7.** Some of the representative images that were holographically recorded and later retrieved from the photorefractive  $\text{LiNbO}_3$  crystal in the lab. (a) Jupiter, (b) horse head nebula, (c) backwards spiral galaxy NCG 4622, (d) galaxy M81, (e) spiral galaxy NGC 4414 and (f) a picture of the Earth taken from the space.

- The polarizer and analyzer were placed in parallel configuration which results in large image modulation depth (seen from figures 2 and 3) and better contrast. In addition, the orientation  $\theta_1 = \theta_2 = 0^\circ$  was chosen to minimize the effect of optical birefringence and phase retardance on the transmitted image beam [25].
- Strong phase modulation may have an adverse impact on the quality of the image storage. Experimental configurations and control settings resulting in a strong phase modulation are generally avoided. A significant phase change was found to occur at high brightness value ( $B = 255$ ) as shown in separate interferometry-based experimental studies conducted to investigate the phase modulation properties of the SLM [26]. Therefore, the chosen brightness ( $B = 128$ ) also ensures minimal cross coupling between intensity and phase modulation.

We used a well-characterized  $0^\circ$  cut Fe:Ce:Ti-doped  $\text{LiNbO}_3$  crystal to record several astronomical images using spatial and angular multiplexing scheme. The choice of astronomical image is particularly important as the pixel values representing the brightness level of the celestial objects have significantly large range. Prior to the recording, a necessary nonlinear correction  $\gamma$ , as described in the previous section, was applied to the selected astronomical images.

The experimental design of a hologram recording and the reading geometry, details of the imaging optics, exposure schedule, page multiplexing and addressing scheme etc. are given in ref. [27]. Some of the illustrative images read out from our volume holographic database in the lab are shown in figure 7. Images displayed in the first row (a)–(c), for example, were addressed onto the SLM without any

**Table 1.** Best parameter fit of sigmoidal function for crossed (parallel) configuration.

$\theta_1$	Brightness	$s_t$	$s_b$	$r_o$	$w$	$r$ (20% <i>s</i> )	$r$ (80% <i>s</i> )
0°	100	1.12(1.00)	0.02(0.21)	204.2(203.2)	22.2(21.7)	172.4(174.1)	233.9(234.3)
	150	1.01(0.99)	0.04(0.24)	127.4(125.7)	19.4(19.1)	100.6(98.5)	154.2(152.9)
	200	1.00(1.00)	0.04(0.25)	101.4(99.3)	18.7(19.1)	75.5(72.8)	127.3(125.8)
	255	1.00(1.01)	0.06(0.25)	73.7(70.7)	18.9(18.8)	47.5(44.6)	99.8(96.7)
30°	100	1.08(1.00)	0.02(0.08)	192.3(191.6)	22.4(22.3)	161.2(160.3)	223.4(222.1)
	150	1.00(0.99)	0.03(0.11)	118.3(116.2)	19.9(20.3)	90.7(88.0)	146.8(144.4)
	200	0.99(1.00)	0.04(0.12)	91.1(89.7)	19.6(19.1)	63.8(63.1)	118.3(116.2)
	255	0.99(1.01)	0.06(0.13)	62.4(62.1)	18.8(19.0)	36.3(35.8)	88.5(88.4)
45°	100	1.07(1.00)	0.02(0.05)	189.6(187.9)	22.2(21.4)	158.9(158.2)	220.4(217.5)
	150	1.00(0.99)	0.03(0.07)	114.7(112.3)	19.4(19.8)	87.8(84.9)	141.5(139.7)
	200	1.00(-)	0.04(-)	86.8(-)	18.7(-)	60.8(-)	112.7(-)
	255	1.00(1.02)	0.05(0.08)	58.6(59.6)	18.8(19.1)	32.5(33.1)	-(86.1)

alteration while the images in the second row (d)–(f), were pre-processed for the SLM  $\gamma$  correction before the actual recording. In addition to the superior image quality rendered in the latter case, the high-frequency image features are also seen to be well preserved. The demonstrable improvement in the visual image quality in the latter case can be attributed to the SLM corrections made to the corresponding images.

Different applications may require different control settings. The control settings for a given application may also have a certain validity range. For example, in our experience with holographic data storage in the lab, we did not find any visually discernable change when the brightness and contrast setting was changed from 128 to 100 or 150. However, the degradation in the image quality becomes obvious at much larger or much smaller values.

#### 4. Summary

Spatial light modulator is an important component of the holographic data storage system. The r.m.s. voltage signal driving the individual LC cells is proportional to the corresponding pixel gray-level in the image. But the overall light transmission characteristics of LC-SLM are highly nonlinear and exhibit a wide range of variations with different parameter settings.

In this paper we have presented the experimental studies pertaining to the operational characteristics of LC-SLM as a function of several control parameters. The transmission properties of LC2002 model are shown to be strongly influenced by several factors such as the optical orientations of the polarizers, input gray levels of the image and brightness and contrast settings. It is also established that SLM nonlinearities, particularly those characterized by power-law type of response, can be easily corrected by applying the inverse transformation to the input images. The importance of proper characterization and evaluation of LC-SLM device response, in three-dimensional data storage applications was directly demonstrated

from the improved visual image quality of the holographically stored and retrieved data pages that were pre-compensated for SLM nonlinearities.

### Acknowledgement

The authors are extremely grateful to the unknown referee for a detailed and careful review of the paper. Referee's insightful comments and critical assessment have helped us to improve the overall quality and presentations in the revised manuscripts.

### References

- [1] K Takizawa, T Fujii, M Kawakita, H Kikuchi, H Fujikake, M Yokozawa, A Murata and K Kishi, *Appl. Opt.* **36**, 5732 (1997)
- [2] J A Coy, M Zalzarriaga, D F Grosz and O E Martinez, *Opt. Engng* **35**, 15 (1996)
- [3] C Soutar, S E Monroe and J Knopp, *Opt. Engng* **33**, 1061 (1994)
- [4] C Soutar, S E Monroe and J Knopp, Complex characterization of the Epson liquid crystal television, in *Proc. SPIE*, Vol. 1959, pp. 269–277; *Optical pattern recognition IV* edited by David P Casasent (1993), pp. 269–277
- [5] J C Kirsch, D A Gregory, M W Thie and B K Jones, *Opt. Engng* **31**, 963 (1992)
- [6] G T Bold, T H Barnes, J Gourlay, R M Sharples and T G Haskell, *Opt. Commun.* **148**, 323 (1998)
- [7] D A Gregory, J C Kirsch and E C Tam, *Appl. Opt.* **31**, 163 (1992)
- [8] X Xun, X Chang and R Cohn, *Opt. Exp.* **12**, 260 (2004)
- [9] A Miniewicz, A Gniewek and J Parka, *Opt. Mater.* **21**, 605 (2003)
- [10] G G Yang and S E Broomfield, *Opt. Commun.* **124**, 345 (1996)
- [11] H-Y Tu, C-J Cheng and M-L Chen, *J. Opt. A: Pure and Appl. Opt.* **6**, 524 (2004)
- [12] P Birch, R Young, D Budgett and C Chatwin, *Opt. Lett.* **26**, 920 (2001)
- [13] R L Eriksen, P C Mogensen and J Glückstad, *Opt. Commun.* **187**, 325 (2001)
- [14] K D Wulff, D G Coleand, Robert L Clark, R DiLeonardo, J Leach, J Cooper, G Gibson and M J Padgett, *Opt. Express* **14**, 4169 (2006)
- [15] J Leach, K Wulff, G Sinclair, P Jordan, J Courtial, L Thomson, G Gibson, K Karunwi, J Cooper, Z J Laczik and M Padgett, *Appl. Opt.* **45**, 897 (2006)
- [16] C Cheng and M Chen, *Opt. Commun.* **237**, 45 (2004)
- [17] J Glückstad, D Palima, P J Rodrigo and C A Alonzo, *Opt. Lett.* **32**, 3281 (2007)
- [18] M Reicherter, S Zwick, T Haist, C Kohler, H Tiziani and W Osten, *Appl. Opt.* **45**, 888 (2006)
- [19] J Hahn, H Kim, Y Lim, G Park and B Lee, *Opt. Express* **16**, 12372 (2008)
- [20] E J Haellstig, L Sjoqvist and M Lindgren, *Opt. Engng* **42**, 613 (2003)
- [21] J L Sanford, P F Grier, K H Yang, M Lu, R S J Olyha, C Narayan, J A Hoffnagle, P M Alt and R L Melcher, *IBM J. Res. Develop.* **42**, 411 (1998)
- [22] D B Glenn and R R Edward, *J. Opt. A: Pure and Appl. Opt.* **27**, 2940 (1988)
- [23] B E A Saleh and M C Teich, *Fundamentals of photonics* (John Wiley & Sons, Inc., 1991), 1st ed.
- [24] A Yariv and P Yeh, *Optical waves in crystals* (Wiley, New York, 1984)
- [25] K Lu and B E A Saleh, *Opt. Engng* **29**, 240 (1990)
- [26] R K Banyal, *Data storage and retrieval using photorefractive crystals*, Ph.D. Thesis, web location: <http://prints.iap.res.in/bitstream/2248/826/1/Thesis.pdf>
- [27] R K Banyal and B R Prasad, *Opt. Commun.* **274**, 300 (2007)